

# MODIFICATIONS OF ELECTRON LINEAR ACCELERATORS PRODUCED IN NIEFA FOR STERILIZATION

Yu.V. Zuev, A.P. Klinov, A.S. Krestianinov, O.L. Maslennikov, V.V. Terentyev  
JSC NIEFA, St. Petersburg, Russia

## Abstract

The paper analyses modifications of electron linear accelerators equipped with one and the same accelerating structure produced in NIEFA. The structure operates in the standing-wave mode at a frequency of 2856 MHz. The accelerators are designed for electron beam processing and provide beam energies in the range of 8-11 MeV and beam average powers up to 10-12 kW.

## INTRODUCTION

A variety of facilities for radiation sterilization with a beam of accelerated electrons was designed and manufactured in NIEFA [1,2]. The paper outlines features of UELR-10-10S [2,6], UELR-10-10T [3], UELR-10-15S [4], LAE10/15 [5] accelerators, in which one and the same accelerating structure is used. The accelerators differ in microwave power sources, electron guns, beam scanning and extraction devices, composition and arrangement of auxiliary systems, consequently, in operational parameters and cost.

## ACCELERATING STRUCTURE

All the listed above accelerators employ a biperiodic electrodynamic structure, which consisting of forty five cells placed on one axis, Fig. 1. The first ten cells form a 5-gap buncher, which provides high capture of beam in the acceleration (up to 85% of the continuous beam) and implements the beam focusing with the RF field.

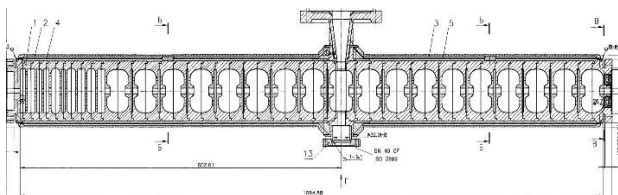


Figure 1: Layout of the accelerating structure.

Cells of the bunching part are cylindrical and U-shaped with a 3.5 mm-thick separating wall. The diameter of beam apertures in the first 4 cells of the buncher is 8 mm, and that in all the rest cells of the structure is 10 mm.

A regular part of the structure consists of  $\Omega$ -shaped accelerating cells alternating with short (4 mm long) cylindrical coupling cells. Calculated values of the Q-factor and shunt-impedance of the accelerating cells are 14800 and 2.9 M $\Omega$ , respectively.

RF coupling of the cells is carried out by pairs of azimuthal slots. The working,  $\pi/2$ , mode of the accelerating field oscillations is excited at a frequency of  $f_0=2856$  MHz. The RF power is input to the structure

through cell # 27, matching iris aperture and wave transformer. The accelerating structure length is 1.1m.

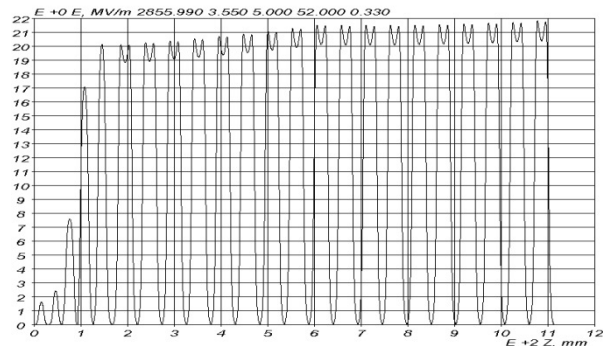


Figure 2: Field distribution on the structure axis.

The nominal distribution of the electric field in the structure is shown in Fig. 2, the energy spectrum corresponding to this field is given in Fig. 3. The electron spectrum width is not more than  $\pm 3\%$ . The designed beam injection energy is 50 keV.

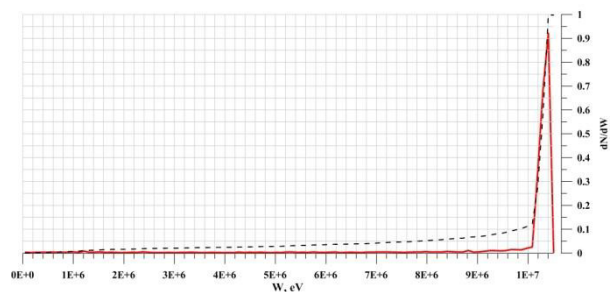


Figure 3: Energy distribution of electrons at the structure output (red solid line) and its integral (black dashed line).

## THERMAL LOAD OF THE STRUCTURE

Thermal stability of the structure is maintained by a cooling jacket made of non-stainless steel and welded to the structure. To compensate the temperature non-uniformity along the structure, the cooling jacket is made double with oppositely directed water flows.

Table 1 demonstrates results of thermal and structural analysis of the structure for 2 values of the average RF power,  $P_W^{avr}$ , dissipated on the walls. Data in the table were calculated for water input temperature of 20°C and are designated as follows:  $Q_W$  is the cooling water flow rate,  $\Delta T_W$  is the water heating,  $\Delta P_W$  is the pressure drop,  $T_{MAX}$  is the maximum temperature and  $\Delta L_{MAX}$  is the maximum displacement (strain).

Table 1: Thermoanalysis Data

$P_{W}^{avr}$ , kW	7.44	11.16	11.16
$Q_W$ , l/min	50	50	75
$\Delta T_W$ , °C	2.1	3.2	2.1
$\Delta P_W$ , atm	0.2	0.2	1.0
$T_{MAX}$ , °C	48.2	61.5	54.4
$\Delta L_{MAX}$ , $\mu$	19	28	22

The distribution of the maximum temperature over the structure cells is given in Fig. 4. The highest level of temperature and thermal deformations can be seen in the area of the maximum heat load and occurs in the 4<sup>th</sup> cell of the buncher [7]. Typical distributions of temperature and thermal deformations within  $\Omega$ -shaped cell of the structure are shown in Fig. 5.

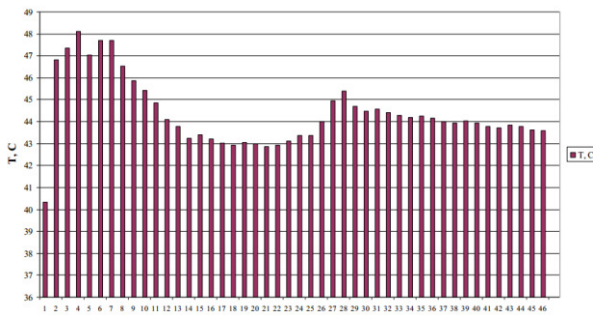


Figure 4:  $T_{MAX}$  distribution over the structure cells at  $P_{W}^{avr}=7.44$  kW и  $Q_W=50$  l/min.

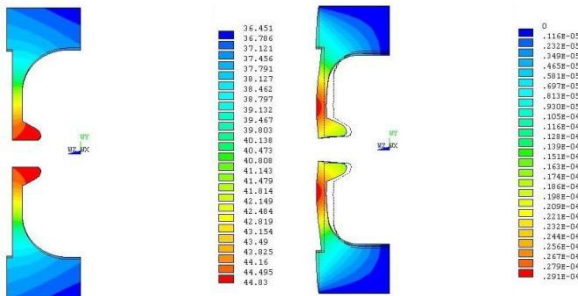


Figure 5: Typical distributions of temperature (left) and thermal deformations (right, 100:1 scale) within 1 cell of the structure.

## RF POWER SYSTEMS

Table 2 shows parameters of RF power sources, which can be used for excitation of our structure and have been previously used in the accelerators. Only one device from the listed makes possible feeding the accelerator gun from the klystron modulator, hence, saving on cost. The preference of the other devices is higher average RF power,  $P_{RF}^{avr}$ , but high anode voltage,  $U_A$ , requires an additional expense for providing the breakdown strength.

ISBN 978-3-95450-181-6

The composition, arrangement, operating parameters and cost of an accelerator mostly depend on a chosen microwave source and accelerating structure.

Table 2: Klystrons with  $f_0=2856$  MHz

Model / manufacturer	$P_{RF}^{puls}$ , MW	$P_{RF}^{avr}$ , kW	$T^{puls}$ , $\mu$ s	$U_A$ , kV
KIU-147A "Toriy", Russia	6	25	16	50
"Belka" "Toriy", Russia	6	60	10	120
TH-2158 THALES, France	5	45	25	122
TH-2173F THALES, France	5	36	26	122
VKS-8262F CPI, USA	5	36	16.3	125

Table 3 shows the accelerator design data in relation to the microwave source used. Operating parameters are designated as follows:  $W_B$  is the beam energy,  $P_B^{avr}$  is the average power of an accelerated beam;  $P_{INP}^{puls}$  ( $P_{INP}^{avr}$ ) is the pulse (average) power supplied to the accelerating structure input;  $T_{RF}$  ( $T_B$ ) is the RF (beam current) pulse duration,  $f_{\Pi}$  is the pulse repetition rate,  $I_B^{acc}$  ( $I_B^{inj}$ ) is the pulse current of an accelerated (injected matched) beam.

Table 3: Accelerator Design Data

Klystron	TH-2158	KIU-147A
$P_B^{avr}$ , kW	10-15	$\geq 10$
$W_B$ , MeV	10	10
$P_{INP}^{puls}$ , MW	3.7	4.7
$P_{INP}^{avr}$ , kW	27.8	22.5
$T_{RF}$ , $\mu$ s	25	16
$T_B$ , $\mu$ s	23	$\geq 14$
$f_{\Pi}$ , Hz	300	300
$I_B^{acc}$ , mA	210	300
$I_B^{inj}$ , mA	280	350

In all the accelerators an AFC circuit is used to keep the operating frequency of the klystron tuned to the resonant frequency of the accelerating structure. The circuit is connected to a port of a ferrite circulator, which protects the klystron against the RF power reflected from the structure.

## PULSE MODULATOR SYSTEMS

The high-voltage pulses necessary to drive the klystron and the accelerator gun are provided by both a solid-state modulator and a conventional line-type modulator on the basis of thyratron and PFN. The quality of formed pulses (top flatness, rise and fall time, remaining ripple, reliability and rightness of synchronization) affects significantly the accelerator performance, including an effective (time-averaged) electron energy spectrum, heat loss and background radiation.

If a klystron and accelerator diode gun have a common modulator, the head and rear parts of the beam pulse are injected to the structure with an improper accelerating field. As a result, an appreciable part of electrons does not acquire a required energy and strikes the vacuum chamber walls, notably, in the vicinity of the beam scanner magnet. The relative contribution from this phenomenon to energy loss depends on the ratio of the transient processes time to the pulse duration.

### ELECTRON SOURCES

First accelerators for sterilization were equipped with diode guns followed by a beam current regulator (a short shielded solenoid, behind which a beam-limiting diaphragm was installed). Later on, diode guns were replaced for standard triode-type sources. The triode guns produced electron beam with an excess of current, but the beam was not well matched with the accelerating structure. This caused an increased loss of electrons both in the accelerating structure and in the gap of the beam scanning magnet. We had to install solenoidal lenses for additional beam focusing in the initial part of the structure and to solve the problem with the magnet vacuum chamber cooling.

At the present time the accelerators intended for sterilization are equipped with specially designed diode or triode electron sources. The sources provide an optimal injection into the structure and a minimum emittance of the beam, Fig. 6 [8]. The accelerators have no need of any external devices for beam focusing.

### BEAM SCANNING SYSTEMS

In the most facilities considered in the paper, the accelerated beam extracted into the atmosphere is scanned over an area 800x20 mm in size. The scanning action results from passing the beam through the gap of a dipole magnet driven by a current waveform repeated in time with a frequency of 1-5 Hz. As a rule the scanning magnet is added with a device based on electric or permanent magnets to compensate the beam angular divergence. In special cases a two-sided irradiation is provided, for example in [4].

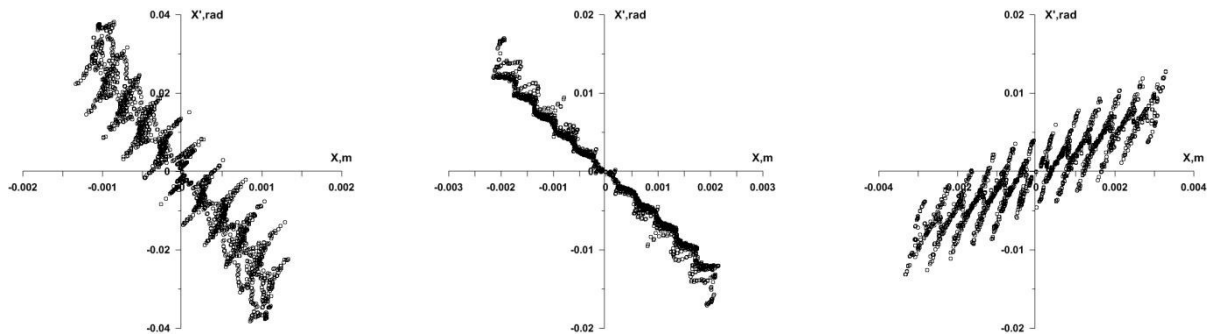


Figure 6: The beam-phase-space portraits at the output of the grid-controlled gun;  $I_B^{inj}=140, 350 700$  mA (from left to right).

### CONCLUSION

To date, nine accelerating structures under discussion have been manufactured. The accelerators equipped with these structures, Fig.7, are compact, have rather low manufacturing, operation and service costs. These machines have been used for electron beam sterilization of medical disposables and food processing over ten years. This year the latest accelerator in question was delivered for exploitation.



Figure 7: The UELR-10-10S accelerator in an assembling room.

### REFERENCES

- [1] M. Vorogushin et al., Problems of atomic science and technology. 2004. №2. Series: Nuclear Physics Investigation (43), p.208-211.
- [2] M. Vorogushin et al., RuPAC'04, Dubna, THJO04, p.112 (2004); <http://www.JACoW.org>.
- [3] M. Demsky et al., RuPAC'06, Novosibirsk, MOLP19, p.372 (2006); <http://www.JACoW.org>.
- [4] M. Demsky et al., RuPAC'12, St. Petersburg, WEPPC052, p.547 (2012); <http://www.JACoW.org>.
- [5] Z. Zimek et al., IAEA Publication SM-EB-31, Vienna (2009); <http://www-pub.iaea.org/>
- [6] M. Vorogushin et al., RuPAC'12, St. Petersburg, FRXCH01, p.167 (2012); <http://www.JACoW.org>.
- [7] V. Tanchuk, S. Grigoriev, NIIIEFA Internal Report, St. Petersburg (2003).
- [8] Yu. Zuev, IVECS-ICEE'14, St. Petersburg, p.308 (2014); IEEE Catalog number CFP14VES-PRT.